Suppression of the skin effect in RF transmission lines via gridded conductor fibers

Ian A. D. Williamson[1], Thien-An N. Nguyen[1], and Zheng Wang[1]
[1]Department of Electrical and Computer Engineering, Microelectronics Research Center, The University of Texas at Austin, Austin, Texas 78758 USA

Supplementary Material

Internal inductance reduction by conductor division

Figure S1 demonstrates how the *internal* inductance is reduced by dividing conductors into smaller subsections.

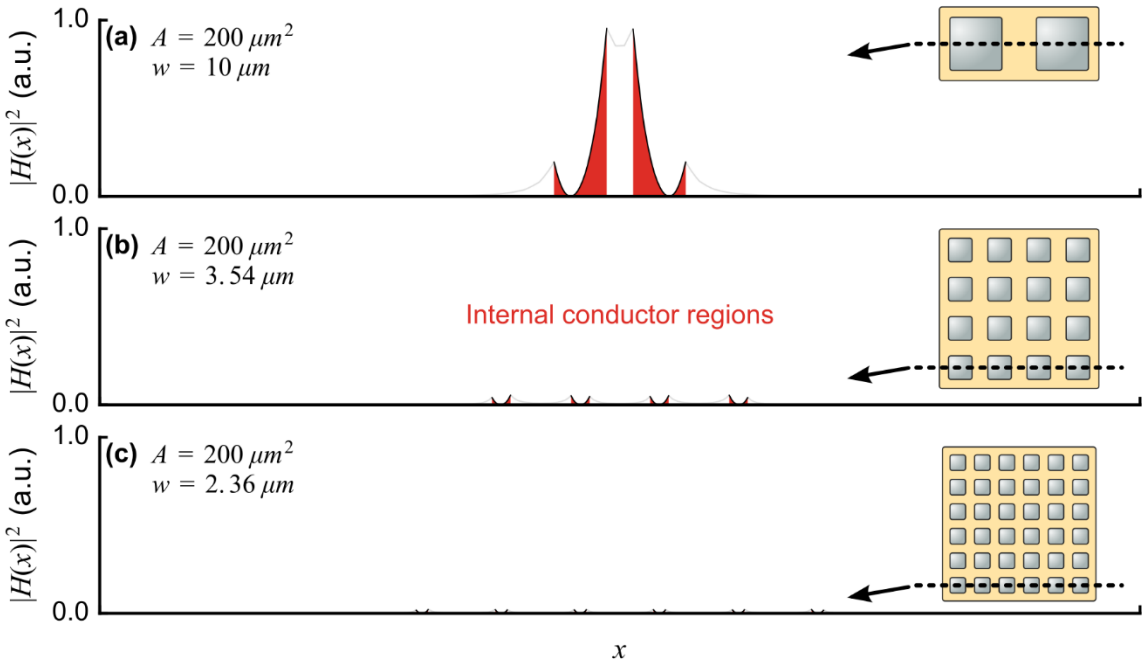

Figure S1 – Profile of $|H|^2$ for (a) 2x1, (b) 4x4, and (c) 6x6 conductor transmission line configurations. Current phasing in the 4x4 and 6x6 is in a checkerboard configuration and all three lines have an equivalent conduction area. Red shaded regions correspond to the result of $\iint |H|^2 dA$ over the "internal" conductor region. The x- and y-ranges for (a), (b), and (c) are equivalent.

Gridded fiber and twisted pair mode energy distribution

Figure S2 compares the magnetic energy distribution of the TEM mode on the twisted pair and a 4x4 gridded fiber at low (100 MHz) and high frequencies (1 GHz). The low and high frequency profiles of the gridded fiber are nearly equivalent whereas the high frequency twisted pair profile exhibits a significant redistribution of the magnetic flux from the conductors towards the surrounding dielectrics due to the skin and proximity effects.

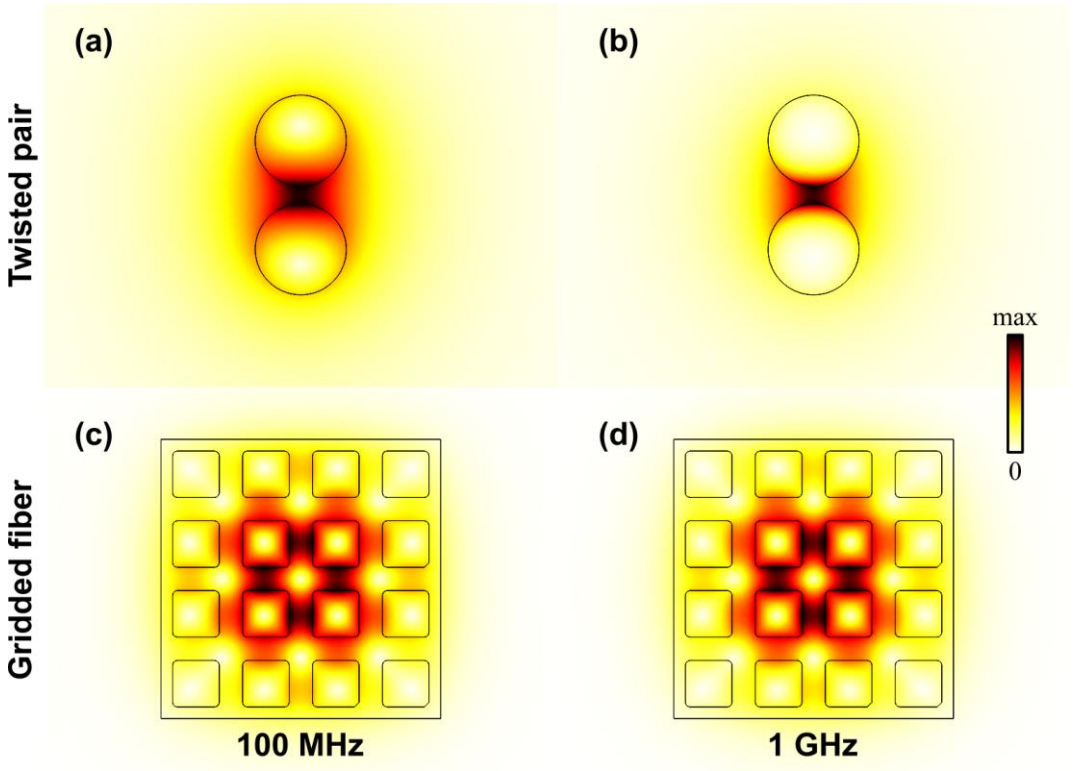

Figure S2 – Magnetic energy distribution for the modes at low (100 MHz) and high (1 GHz) frequencies for the gridded fiber and twisted pair. The parameters used for each structure are equivalent to those used in Figure 1 of the main text.

Internal inductance percentage of total inductance

Figure S3 shows the ratio of the internal inductance to the total inductance for the gridded fiber and twisted pair as a function of the *high frequency characteristic impedance*, which is varied by tuning the relative conductor separation.

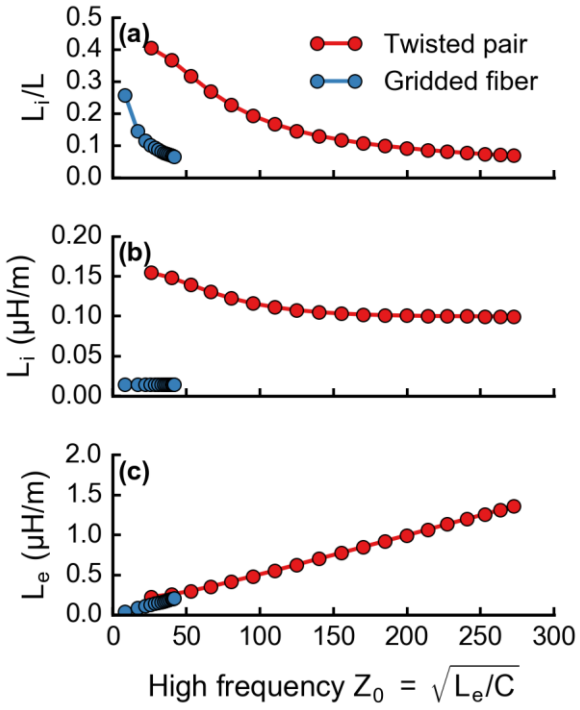

Figure S3 – (a) Ratio of internal inductance to total inductance, (b) internal inductance, and (c) external inductance all plotted as a function of the high frequency characteristic impedance. The HF characteristic impedance is varied by increasing the relative conductor separation.

Transmission line modeling

The phase and attenuation spectra, $\beta(\omega)$ and $\alpha(\omega)$, in the main text correspond to the real and imaginary components of the complex eigenvalues computed by a COMSOL Multiphysics eigenmode simulation. The per-unit length circuit parameters used throughout this paper were numerically computed from modal field distributions produced by the eigensolver. Their definitions are given by:

$$L(\omega) = \frac{\mu}{|I_0|^2} \iint |\overline{H}|^2 \, ds \tag{S1}$$

$$C = \frac{\varepsilon}{|V_0|^2} \iint |\overline{E}|^2 \, ds \tag{S2}$$

$$R(\omega) = \frac{1}{|I_0|^2} \iint \sigma \left|\overline{E}\right|^2 ds \tag{S3}$$

Note that we have assumed all dielectric materials to be lossless.

$|I_0|$ corresponds to the total "outgoing" or "incoming" current, and is computed by integrating the quantity $|J_z|$ over the entire conductor area and dividing by two. $|V_0|$ is calculated for the twisted pair by integrating the electric field along a path from the surface of one conductor to the other; for the gridded fiber, the voltage cannot be calculated from the model. In this paper we have not shown any calculated capacitance because we have primarily focused on resistive and inductive effects. However, the capacitance of the gridded fiber could be computed through an electrostatic simulation of the gridded fiber or with the complex propagation constant and *R* and *L*. We have verified that these two methods are in agreement for the structures considered in this paper.

Figure S4 depicts a schematic of (a) the gridded fiber simulation domain and (b) the twisted pair simulation domain. The simulated gridded fiber resembles its depiction in Fig. 1 and both geometries use sufficiently spaced PEC boundaries. The simulated twisted pair geometry differs from its usual form in that it does not have the thin dielectric coating. In practice, the thin coating is challenging to accurately mesh, especially for the narrow conductor separations considered in this work. In our models we completely fill the domain with dielectric to improve the simulation performance and also so that equation (S4) can be used to accurately predict the characteristic impedance of the line.

$$Z_{TP} = \frac{120}{\sqrt{\varepsilon_r}} \operatorname{arccosh}\left(\frac{S}{D}\right) \tag{S4}$$

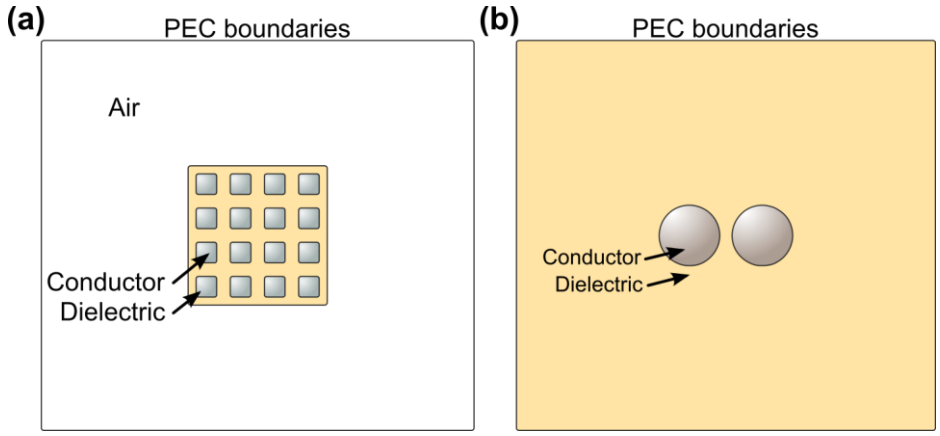

Figure S4 – Schematic of computational domain for the (a) gridded fiber and (b) twisted pair transmission lines.

Reduced conductivity performance scaling

Figure S5 shows that the LC regime of the prototype Bi-Sn fiber shown in the inset of Fig. 2a has an LC regime frequency range (Figure S5, blue curves) that is increased by a factor $1/0.045 = 22.2$ from the Cu conductor fiber simulated in Fig. 1 (Figure S5, red curves). By enlarging the dimensions of the Bi-Sn fiber by a factor of $\sqrt{22.2} = 4.7$, performance equivalent to that of the Cu conductor fiber can be obtained.

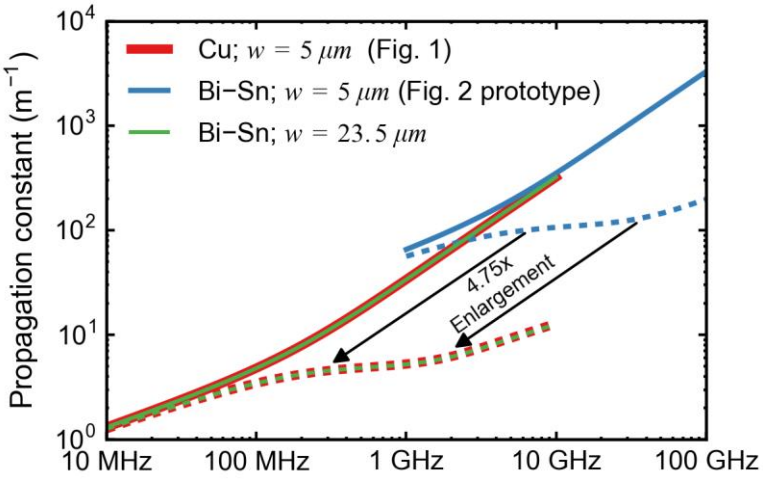

Figure S5 – Computed $\beta(\omega)$ (solid lines) and $\alpha(\omega)$ (dashed lines) for a copper conductor gridded fiber that is identical to the structure in Fig. 1, a Bi-Sn fiber identical to the prototype shown in Fig. 2, and a Bi-Sn fiber that has been enlarged from the prototype by a factor of 4.7 to achieve a performance equivalent to that of the Cu design. All fibers have $a/w = 5$.